DRAFT VERSION APRIL 24, 2003
Preprint typeset using LaTeX style emulateapj v. 19/02/01

CLUES ON THE EVOLUTION OF THE CARINA DWARF SPHEROIDAL GALAXY FROM THE COLOR DISTRIBUTION OF ITS RED GIANT STARS [1]

LUCA RIZZI,[2,3] ENRICO V. HELD,[2] GIANPAOLO BERTELLI,[4,2] IVO SAVIANE[5]
Draft version April 24, 2003

ABSTRACT

The thin red giant branch (RGB) of the Carina dwarf spheroidal galaxy appears at first sight quite puzzling and seemingly in contrast with the presence of several distinct bursts of star formation. In this *Letter*, we provide a measurement of the color spread of red giant stars in Carina based on new *BVI* wide-field observations, and model the width of the RGB by means of synthetic color-magnitude diagrams. The measured color spread, $\sigma_{V-I} = 0.021 \pm 0.005$, is quite naturally accounted for by the star-formation history of the galaxy. The thin RGB appears to be essentially related to the limited age range of its dominant stellar populations, with no need for a metallicity dispersion at a given age. This result is relatively robust with respect to changes in the assumed age-metallicity relation, as long as the mean metallicity over the galaxy lifetime matches the observed value ([Fe/H]= -1.91 ± 0.12 after correction for the age effects). This analysis of photometric data also sets some constraints on the chemical evolution of Carina by indicating that the chemical abundance of the interstellar medium in Carina remained low throughout each episode of star formation even though these episodes occurred over many Gyr.

Subject headings: galaxies: individual (Carina) — galaxies: dwarf — galaxies: evolution — galaxies: stellar content — Local Group

1. INTRODUCTION

Since its discovery in 1977 (Cannon, Hawarder, & Tritton can+77), the Carina dwarf spheroidal (dSph) galaxy has played an important role in our understanding of the nature of dwarf galaxies. Carina was in fact the first dSph galaxy in which a prominent intermediate age population was recognized (Mould & Aaronson mou+aar83). The presence of a non-negligible component of old stars was subsequently revealed by the detection of a large number of RR Lyrae variable stars (Saha, Monet, & Seitzer sah+86; Dall'Ora et al. dall+03). Mighell (migh90) estimated the old population to constitute (17 ± 4)% of the galaxy population, a number confirmed by Smecker-Hane et al. (smec+94) and Mighell (migh97). A detailed description of the star-formation history (SFH) of Carina was given by Smecker-Hane et al. (smec+94, smec+96). A deep *BR* color-magnitude diagram (CMD) revealed the presence of three distinct turn-offs, pointing at three separate episodes of star formation approximately 2, $3-6$ and $11-13$ Gyr ago (see also Monelli et al. mone+03). A quantitative assessment of this scenario was then provided by CMD simulation techniques applied to CTIO 4m and HST data (Hurley-Keller, Mateo, & Nemec hurl+98; Hernandez, Gilmore, & Valls-Gabaud her+00; Dolphin dol02).

Quite surprisingly given this complex star-formation history, Carina shows a *very thin red giant branch* with all the different turn-offs connecting at the RGB base (Smecker-Hane et al. smec+94, smec+96). This seems to imply that either no significant metal enrichment took place in Carina, or that age and chemical enrichment of the stellar populations played in opposite directions to yield a narrow RGB. While these alternative views have often been discussed, they have never been quantitatively addressed. The chemical evolution of dwarf spheroidal galaxies, in particular the role of galaxy-wide gas outflows and/or infall, remains a controversial issue and many basic questions are still open. Recent efforts to model the chemical evolution of dwarf spheroidal galaxies have been presented by Ikuta & Arimoto (ikut+arim02), Carigi, Hernandez, & Gilmore (cari+02), and Tolstoy et al. (tols+03). All groups use known SFHs to infer the chemical-enrichment histories of dSph galaxies, but the scenarios differ in the role played by galactic winds and gas infall.

This *Letter* shows that realistic modeling of the color distribution of red giant stars by population synthesis methods can help constraining the chemical evolution of dwarf spheroidals galaxies. The intrinsic color width of the upper RGB in Carina is quantified here by exploiting the high statistics of a new *BVI* database from wide-field observations. The star-formation history of Carina is then derived for a set of different metal-enrichment histories (the age-metallicity relation of this galaxy is still uncertain) by comparing observed and synthetic color-magnitude diagrams. The narrow RGB of Carina is shown to be consistent with the star-formation history derived from the observed CMDs, under reasonable assumptions on the chemical-enrichment history.

2. THE DATA

Observations of Carina were carried out using the *Wide Field Imager* at the ESO/MPG 2.2m telescope. The camera consists of a mosaic of eight 2k $\times$ 4k EEV CCDs, in a square array of 2 $\times$ 4 detectors. In this configuration, the total number of pixels is 8k $\times$ 8k, with a scale of 0.238 arcsec pixel^{-1} and a field of view $32' \times 32'$. Three different fields were observed: a central field and two outer fields with $\sim 20'$ offsets. Sky conditions

[1] Based on data collected at E.S.O. La Silla, Chile, Proposals No. 63.N-0017 and 64.N–0512

[2] INAF, Osservatorio Astronomico di Padova, vicolo dell'Osservatorio 5, I-35122 Padova, Italy; (held,rizzi)@pd.astro.it

[3] Dipartimento di Astronomia, Università di Padova, vicolo dell'Osservatorio 2, I-35122 Padova, Italy

[4] Istituto di Astrofisica Spaziale e Fisica Cosmica, CNR, Area di Ricerca Tor Vergata, Via del Fosso del Cavaliere 100, 00133 Roma, Italy

[5] European Southern Observatory, Casilla 19001, Santiago 19, Chile

were photometric, and standard star fields taken from the list of Landolt (lan92) were observed for calibration purpose. A full description of the data and reduction methods will be presented in a forthcoming paper (E. V. Held et al. 2003, in prep.) while just a brief outline is given here. Pre-reduction of CCD images was performed within the IRAF environment. Each image was bias-subtracted and flat-fielded using twilight sky flats. After these steps, all images were astrometrically calibrated using the IRAF MSCRED package (Valdes vald98) and the script package WFPRED developed at the Padova Observatory.

Photometry was obtained using DAOPHOT II/ALLSTAR (Stetson ste87) on the co-added images, and the results were calibrated using calibration relations computed from standard stars observed in all CCDs. Similarly, aperture corrections were computed using a growth curve analysis performed on bright isolated stars in each CCD. Artificial star tests were done to evaluate the uncertainty of photometry and the degree of completeness of the data. The photometric errors in the V band range from ~ 0.01 mag near the tip of the RGB, to ~ 0.3 mag near the detection limit.

3. MODELING THE RED GIANT BRANCH OF CARINA

3.1. *RGB width measurement*

These wide field data allowed us to obtain a sound quantitative estimate of the RGB width in Carina. In order to measure the color spread of the RGB, a fiducial ridge line was fitted to the mean colors of red giants in 0.5 mag bins. The distribution of color residuals about the fiducial line was then measured down to 1.5 mag below the tip. After quadratic subtraction of the contribution of photometric errors, the estimated intrinsic color spread of the upper RGB is:

$$\sigma_{(V-I)} = 0.021 \pm 0.005$$

where the statistical error was estimated by bootstrap resampling of the RGB sample in 500 trials.

Using a direct comparison of the red giant branch of Carina with the ridge lines of Galactic globular clusters (Da Costa & Armandroff dac+arm90), we estimated a mean metallicity [Fe/H] = –2.08 ± 0.12 on the Zinn & West (zinn+west84) scale (E. V. Held et al. 2003, in prep.). This value agrees well with previous photometric determinations (Mould & Aaronson mou+aar83; Mighell migh90; Smecker-Hane et al. smec+94; Mateo, Hurley-Keller, & Nemec mat+hur98), as well as the low dispersion spectroscopic measurements of the Ca II lines of Da Costa (dac94) and Smecker-Hane et al. (smec+99). A somewhat higher metallicity, [Fe/H] = –1.6 with a spread of 0.5 dex, has recently been derived by Tolstoy et al. (tols+03) from high-resolution spectroscopy of 5 red giant stars.

The difference between this new spectroscopic estimate and previous photometric [Fe/H] value can be only partly accounted for by age effects on the RGB color. The stars in Carina are, in fact, ~ 7 Gyr younger than the stellar populations of Galactic globular clusters (see below), and we know that younger isochrones are shifted blueward (see, e.g., Da Costa daco98). Using Girardi's et al. (gira+00) models in the range $Z = 0.0001$ to 0.0004, we find the effects of a younger age on the $(V-I)$ color to be ~ 0.035 mag at the RGB level used for metallicity estimation. This bluer color mimics a lower metallicity, by ~ 0.17 dex (see also Smecker-Hane et al. smec+94). By taking this effect into account, the age-corrected metallicity of Carina is then [Fe/H]= –1.91 ± 0.12.

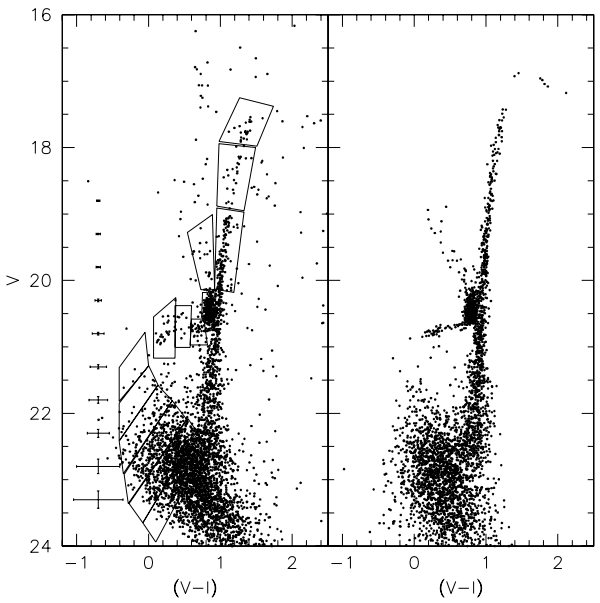

FIG. 1.— Comparison of the observed and synthetic color-magnitude diagrams for Carina. The *left* panel shows the statistically decontaminated CMD of the central region of Carina, along with the boxes used by the χ^2 minimization technique. The *right* panel shows the simulated color-magnitude diagram, assuming the PT law described in the text.

The color distribution of RGB stars formally corresponds (for an old population) to a metallicity dispersion $\sigma_{[Fe/H]} = 0.10 \pm 0.04$, which is significantly smaller than the quoted dispersion of spectroscopic measurements.

3.2. *Population synthesis*

Figure 1 (left panel) shows the CMD of the the central part of Carina, for which simulations were performed. An elliptical region with a 12 arcmin semi-major axis, 65° position angle, and 0.33 ellipticity (Irwin & Hatzidimitriou irw+hat95) was selected to this purpose. The intrinsically poor statistics of the red giant stars in Carina prevents reliable measurements of the RGB width in the outer regions. The observed CMD was simulated using a parametric technique similar to that employed by Aparicio, Gallart, & Bertelli (apa+97a), and a description of our methods is presented by Rizzi et al. (riz+01). In brief, our technique assumes a number of known input parameters, such as the initial mass function (IMF), the distance to the galaxy, and the reddening. A Salpeter (sal55) IMF is adopted, since recent work suggests a general validity of this IMF for masses larger than $0.5 M_{\odot}$ (Scalo sca98; Kroupa kro00). A distance modulus $(m-M)_0 = 20.00 \pm 0.06$ and a reddening $E(B-V) = 0.045 \pm 0.01$ were adopted (E. V. Held et al. 2003, in prep.). Using these input parameters, a set of synthetic stellar populations were generated using models from the library of Girardi et al. (gira+00) and the simulation code ZVAR that linearly interpolates the evolutionary tracks both in age and metallicity, including the effects of binary stars. The observational effects were applied to the theoretical random populations using the photometric errors and completeness obtained from the results of artificial star experiments.

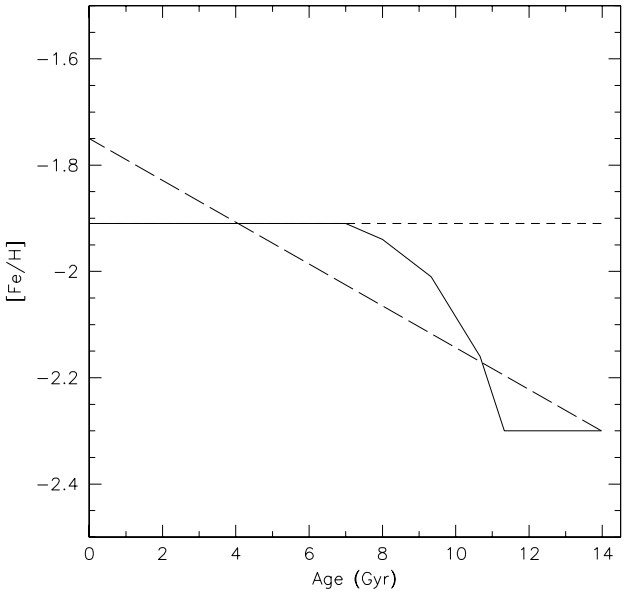

FIG. 2.— The different chemical-enrichment histories tested in this work. The *continuous line* represents the adopted PT law, while the *long-dashed* and *short-dashed* lines show the linear and constant laws, respectively.

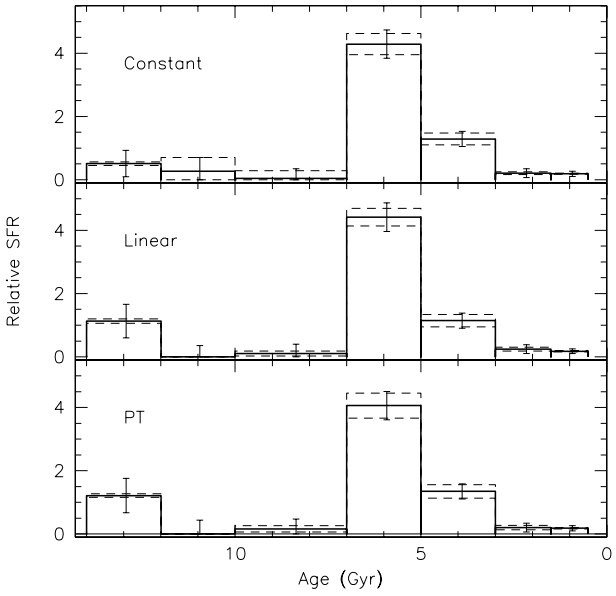

FIG. 3.— Relative star-formation history for the central region of Carina. The rates are normalized to a lifetime average rate of 25.6 $M_{\odot}$ Myr^{-1}. The error bars represent 3σ confidence intervals from the chi-square statistic, while *dashed lines* show the upper and lower limits to the SFH derived from 100 repeat CMD simulations. The bulk of the star formation appears to have happened in a long episode between ~ 3 and ~ 7 Gyr ago.

A basic ingredient of the simulation is the chemical-enrichment history (CEH), for which we chose to test a number of reasonable assumptions (Fig. 2). The first tested law is characterized by a prompt initial enrichment at ages of $\sim$ 12 Gyr, which is responsible for producing much of the observed metals, followed by a slow metallicity increase leading to a final value of [Fe/H] ~ -1.9 (hereafter "PT law", after the age-metallicity relation modeled by Pagel & Tautvaisiene pag+tau98 for the Large Magellanic Cloud). This trend is similar to the CEH recently derived from spectroscopic observations of dwarf spheroidal galaxies (Gallart et al. gal+02; Tolstoy et al. tols+03). The final metallicity was constrained to yield *a mean metallicity over the galaxy lifetime equal to the value derived from the photometry of Carina*. This was done iteratively since the galaxy's star-formation history is affected by the CEH normalization, and vice versa.

Other tested laws, illustrated in Fig. 2, include a constant metallicity law at [Fe/H] = –1.91 and a linear law starting at [Fe/H] = –2.3 and reaching [Fe/H] = –1.76 at the present epoch. These laws sample a wide range of possibilities in the rate of metal enrichment, still yielding the correct mean [Fe/H] over the SFH. Other chemical evolution laws with a more metal-rich normalization would be inconsistent with the photometric data.

A total of 7 populations were generated using these input laws, with age bins centered at 1, 2.25, 4, 6, 8.5, 11 and 13 Gyr, each bin containing 30.000 stars. Tests were made with both a 30% fraction of binary stars and no binaries at all. The SFH that best fits the observed color-magnitude diagram was found by comparing the number of real and simulated stars inside a number of regions in the CMD ("boxes"). These were chosen to map (i) the luminosity function along the main sequence, (ii) the relative contribution of blue and red horizontal branch stars, (iii) the number of "red clump" stars, and (iv) the total number of stars along the RGB (see Fig. 1, left panel). The width of the RGB itself is not an input constraint for the best-fit CMD.

The best fitting synthetic diagram, obtained by minimizing the differences in star counts between the simulated and observed CMD with a downhill χ^2 minimization algorithm, is shown in the right panel of Fig. 1 for the PT law.

The derived star-formation histories are shown in Fig. 3, for the different assumptions on the metal-enrichment history. Our analysis of wide-field data agrees with previous results in that $\sim$ 75% of the stars formed between 3 and 7 Gyr ago, with a small yet significant old stellar component. Note that, although the details of the SFH are different, the main episodes of star formation are relatively independent of the adopted CEH. In fact, our suitable choice of the CMD regions over which stars are counted makes the derived SFH more sensitive to the lifetimes of evolutionary phases than to the metal enrichment law (and uncertainties on the isochrone colors).

3.3. *A thin RGB in Carina*

We can now return to the problem of the origin of the extremely thin RGB in Carina, having in hand the necessary tools to quantitatively evaluate the effects of the chemical-enrichment and star-formation history. The color distribution of simulated RGB stars about a fiducial line was measured for each choice of the CEH, using the same methods as for the real data. We did not make use of the absolute colors of the synthetic RGBs, because of known uncertainties on the isochrone colors. The mean widths measured for the simulated diagrams are $\sigma_{(V-I)} = 0.023 \pm 0.003$ for the linear and constant laws, and $\sigma_{(V-I)} = 0.025 \pm 0.003$ for the PT law. The mean values and statistical errors result from 300 trials. These results are essentially independent of the adopted fraction of binary stars. The simulations thus indicate that *the Carina's narrow RGB naturally arises from the SFH derived from the data*. The results for all the tested enrichment laws agree with the observed color spread within one standard deviation. Indeed, these val-

ues probably mark the lower limit to the measurable RGB width set by stochastic effects and photometric errors in the CMD simulations. As expected, no conclusions can be reached on the details of chemical enrichment from photometry alone. A large sample of spectroscopic measurements will help, provided that it is of the highest precision and accuracy.

4. DISCUSSION AND CONCLUSIONS

In this *Letter*, we have reported new measurements of the mean metallicity ([Fe/H]=–1.91 ± 0.12, after correction for the effects of age) and the color spread (σ_{V-I} = 0.021 ± 0.005) of red giant stars in Carina, based on new wide-field observations. Using synthetic color-magnitude diagrams to model the color distribution of RGB stars, we have quantitatively shown that the thinness of the red giant branch is a direct consequence of the derived star-formation history, for most chemical evolution laws that are plausible and consistent with the observed mean metallicity of the galaxy.

The most fundamental reason for the RGB being so thin is the fact that the predominant intermediate-age stellar population that makes up the RGB, was formed in a limited time interval (5 ± 2 Gyr ago), with only a minor contribution by an old population. In theory, both the age range and the metallicity evolution of the red giant stars contribute in some way to the color range of the RGB, but the effects are subtle and hardly measurable. In fact, (i) the age interval is too small for the isochrone separation to be measurable, and (ii) the sensitivity of the RGB color to changes in [Fe/H] is low for metal-poor systems, so the effect of *modest* metal enrichment during the main star-formation episode is negligible too.

Our photometric analysis bears some interesting implications on the chemical evolution history, by providing evidence that Carina could not experience a significant metal enrichment (i.e. above [Fe/H]~ -1.9), certainly not before 3 Gyr ago. In fact, the lifetime-averaged metallicity inferred from photometric observations definitely rules out a metal-rich final composition. Little information is available on the most recent epoch, because stars younger than $\sim$ 3 Gyr are only a trace population, but for the same reason no significant metal enrichment is expected in the last few Gyr. The most likely scenario remains that indicated by chemical evolution models, in which substantial metal enrichment is associated with the earliest star-formation epoch ($\gtrsim$ 12 Gyr).

In summary, both the episodic star-formation activity (with long-lasting episodes and quiescent phases) and the lack of a significant metal enrichment suggest that metal-enriched gas outflows play a role in the evolution of Carina and other low-mass galaxies (Vader vade86; Mac Low & Ferrara macl+ferr99; see also Gallagher & Wyse gal+wys94; Kunth & Östlin kun+ost00; Carigi et al. cari+02). Closed-box models (e.g., Ikuta & Arimoto ikut+arim02) appear unable to explain the very low metal abundances of dwarf galaxies like Carina. In a similar way, the oxygen abundances measured in the interstellar gas of dwarf irregular galaxies appear hardly consistent with a closed-box model (see, e.g., Saviane et al. savi+02, and references therein). Observational evidence of galactic winds provides support to this scenario for active starbursts, a recent example being the Chandra observation of a metal-enriched galactic wind in the dwarf galaxy NGC 1569 (Martin, Kobulnicky, & Heckman mart+02).

We thank the referee for suggesting some significant improvements to the paper, Drs. L. Carigi and X. Hernadez for helpful remarks, and M. Tosi for useful conversations on dwarf galaxy evolution. Support for this work was provided by the Italian Ministry for University and Research through grants COFIN2001028897 and COFIN2002028935.

REFERENCES

[1997]Aparicio, A., Gallart, C., & Bertelli, G. 1997, AJ, 114, 669
[1998]Da Costa, G. S. 1998, in Stellar astrophysics for the Local Group: VIII Canary Islands Winter School of Astrophysics, eds. Aparicio, A., Herrero, A., and Sanchez, F. (New York : Cambridge University Press), 351
[1977]Cannon, R. D., Hawarden, T. G., & Tritton, S. B. 1977, MNRAS, 180, 82P
[2002]Carigi, L., Hernandez, X., & Gilmore, G. 2002, MNRAS, 334, 117
[1994]Da Costa, G.S. 1994, in Proceedings of the ESO/OHP Workshop on Dwarf galaxies, eds. Georges Meylan and Phillippe Prugniel. (Garching: European Southern Observatory), 221
[1990]Da Costa, G. S., & Armandroff, T. E. 1990, AJ, 100, 162
[2003]Dall'Ora, M. et al. 2003, AJ, in press (astro-ph/0302418)
[2002]Dolphin, A.E. 2002, MNRAS, 332, 91
[2002]Gallart, C., Zinn, R., Pont, F., Hardy, E., Marconi, G., & Buonanno, R. 2002, The Messenger, 108, 16
[1994]Gallagher, J.S., & Wyse, R.F.G. 1994, PASP, 106, 1225
[2000]Girardi, L., Bressan, A., Bertelli, G., & Chiosi, C. 2000, A&AS, 141, 371
[2000]Hernandez, X., Gilmore, G., & Valls-Gabaud, D. 2000, MNRAS, 317, 831
[1998]Hurley-Keller, D., Mateo, M., & Nemec, J. 1998, AJ, 115, 1840
[2002]Ikuta, C., & Arimoto, N. 2002, A&A, 391, 55
[1995]Irwin, M., & Hatzidimitriou, D. 1995, MNRAS, 277, 1354
[2000]Kroupa, P. 2001, MNRAS, 322, 231
[2000]Kunth, D., & Östlin, G. 2000, ARA&A, 10, 1
[1992]Landolt, A. U. 1992, AJ, 104, 340
[1999]Mac Low, M.-M., & Ferrara, A. 1999, ApJ, 513, 142
[2002]Martin, C. L., Kobulnicky, H. A., & Heckman, T. M. 2002, ApJ, 574, 663
[1998]Mateo, M., Hurley-Keller, D., & .Nemec, J. 1998, AJ, 115, 1856
[1997]Mighell, K. J. 1997, AJ, 114, 1458
[1990]Mighell, K. J. 1990, A&AS, 82, 39
[2003]Monelli, M. et al. 2003, AJ, in press (astro-ph/0303493)
[1983]Mould, J., & Aaronson, M. 1983, ApJ, 273, 538
[1998]Pagel, B. E. J., & Tautvaisiene, G. 1998, MNRAS, 299, 535
[2002]Rizzi, L., Held, E.V., Bertelli, G., Nasi, E., Saviane, I., & Vallenari, A. 2002, in ASP Conf. Series, Observed HR diagrams and stellar evolution: The interplay between observational constraints and theory, eds. Thibault Lejeune and Jõao Fernandes (San Francisco: ASP), in press
[1986]Saha, A., Monet, D. G., & Seitzer, P. 1986, AJ, 92, 327
[1955]Salpeter, E. E. 1955, ApJ, 121, 161
[2002]Saviane, I., Rizzi, L., Held, E. V., Bresolin, F., & Momany, Y. 2002, A&A, 390, 59
[1998]Scalo, J. 1998, in ASP Conf. Ser. 142: The Stellar Initial Mass Function (38th Herstmonceux Conference), 201, eds. G. Gilmore and D. Howell (San Francisco: ASP), 201
[1994]Smecker-Hane, T., Stetson, P.B., Hesser, J.E., & Lehnert, M.D. 1994, AJ, 108, 507
[1996]Smecker-Hane, T., Stetson, P.B., Hesser, J.E., & Vandenbergh, D.A. 1996, in ASP Conf. Ser. 98: From Stars to Galaxies: the Impact of Stellar Physics on Galaxy Evolution, eds. C. Leitherer, U. Fritze-von-Alvensleben, and J. Huchra (San Francisco: ASP), 328
[1999]Smecker-Hane, T. A., Mandushev, G. I., Hesser, J. E., Stetson, P. B., Da Costa, G. S., & Hatzidimitriou, D. 1999, in ASP Conf. Ser. 192: Spectrophotometric Dating of Stars and Galaxies, 159, eds. I. Hubeny, S. Heap, and R. Cornett (San Francisco: ASP), 159
[1987]Stetson, P.B. 1987, PASP, 99, 191
[2003]Tolstoy, E., Venn, K. A., Shetrone, M., Primas, F., Hill, V., Kaufer, A., & Szeifert, T. 2003, AJ, 125, 707
[1998]Valdes, F. G. 1998, in ASP Conf. Ser. 145: Astronomical Data Analysis Software and Systems VII, 7, 53, eds. R. Albrecht, R.N. Hook and H.A. Bushouse (San Francisco: ASP), 53
[1986]Vader, J. P. 1986, ApJ, 305, 669
[1984]Zinn, R., & West, M. J. 1984, ApJS, 55, 45